

Semi-flexible compact polymers in two dimensional nonhomogeneous confinement

D Marčetić¹, S Elezović-Hadžić^{2,5} , N Adžić³ and I Živić⁴

¹ Faculty of Natural Sciences and Mathematics, University of Banja Luka, M. Stojanovića 2, Bosnia and Herzegovina

² Faculty of Physics, University of Belgrade, PO Box 44, 11001 Belgrade, Serbia

³ Faculty of Physics, University of Vienna, Boltzmannngasse 5, A-1090 Vienna, Austria

⁴ Faculty of Science, University of Kragujevac, Radoja Domanovića 12, Kragujevac, Serbia

E-mail: dusanka.marcetic-lekic@pmf.unibl.org, suki@ff.bg.ac.rs, natasa.adzic@univie.ac.at and ivanz@kg.ac.rs

Received 24 October 2018, revised 9 January 2019

Accepted for publication 6 February 2019

Published 25 February 2019



CrossMark

Abstract

We have studied the compact phase conformations of semi-flexible polymer chains confined in two dimensional nonhomogeneous media, modelled by fractals that belong to the family of modified rectangular (MR) lattices. Members of the MR family are enumerated by an integer p ($2 \leq p < \infty$) and fractal dimension of each member of the family is equal to 2. The polymer flexibility is described by the stiffness parameter s , while the polymer conformations are modelled by weighted Hamiltonian walks (HWs). Applying an exact recurrence equations method, we have found that partition function Z_N for closed HWs consisting of N steps scales as $\omega^N \mu^{\sqrt{N}}$, where constants ω and μ depend on both p and s . We have calculated numerically the stiffness dependence of the polymer persistence length, as well as various thermodynamic quantities (such as free and internal energy, specific heat and entropy) for a large set of members of the MR family. Analysis of these quantities has shown that semi-flexible compact polymers on MR lattices can exist only in the liquid-like (disordered) phase, whereas the crystal (ordered) phase has not appeared. Finally, behavior of the examined system at zero temperature has been discussed.

Keywords: solvable lattice models, structures and conformations, phase diagrams, polymers

(Some figures may appear in colour only in the online journal)

⁵ Author to whom any correspondence should be addressed.

1. Introduction

Behaviour of a linear flexible polymer in various types of solvents has been extensively studied in the past and the subject is well understood, at least when the universal properties of polymer statistics are under consideration [1]. The canonical model of a linear polymer is the self-avoiding walk (SAW), which is a random walk that must not contain self-intersections. In this model, steps of the walk are usually identified with monomers, while the surrounding solvent is represented by a lattice [2]. In a good solvent (high temperature regime) polymer chain is in extended state, whereas in a bad solvent (low temperatures) it is in compact phase. Since in the compact phase a polymer fills up the space as densely as possible, it is often modelled by Hamiltonian walk (HW), which is a SAW that visits every site of the underlying lattice.

Most of real polymers, especially biologically important ones, are semi-flexible, but contrary to the flexible polymers, knowledge of their conformational properties is scarce. The measure of bending rigidity of a semi-flexible chain is its persistence length l_p , which can be understood as an average length of straight segments of the chain. In a good solvent the stiffness of the polymer only enlarges the persistence length, while in a bad one (when polymer is compact), an increase of the chain stiffness may promote the transition from a disordered phase (when polymer bends are randomly distributed over the polymer, with finite density) to an ordered crystalline phase (when large rod-like parts of the chain lie in parallel order, with zero density of bends). In order to study the compact phase of semi-flexible polymers on homogeneous lattices Flory introduced a model of polymer melting [3], in which a compact polymer is modelled by HW, while the bending rigidity is taken into account by assigning an extra energy to each bend of the chain. Applying the proposed model within the mean-field theory, it has been found [3] that there are two compact phases: disordered liquid-like and ordered crystal-like phase, and a phase transition caused by competition between the chain entropy and the stiffness of the polymer has emerged. At high temperatures, the entropy dominated disordered phase exists, in which the number of bends in the chain is comparable with the total number of monomers, and the persistence length is finite. At low temperatures bending energy dominates, so that polymer takes ordered crystalline form, in which bends exist only on the opposite edges of the underlying lattice. In this phase the persistence length becomes comparable to the lattice size. Using various techniques, in a series of papers [4–12], the existence and nature of phase transition between these two phases of compact polymers have been investigated, giving quite different results for the order of phase transition.

Besides being interesting from the pure physical point of view, semi-flexible compact polymer models are of great importance for better understanding of some biological systems and processes. For example, DNA condensation [13] and protein folding problem [14] take place in squeezed cellular environment and demand for compact states of these rigid polymers. For such systems, coarse-grained polymer models often present valuable tool in explaining the major features observed in experiments [15].

The Hamiltonian walk problem, even in its simplest form, with no interactions involved and on regular lattices, is a very difficult one. Exact enumeration of HWs, which is a prerequisite for further analysis of the compact polymer properties, is limited to rather small lattice sizes. For instance, HWs on L^2 square lattice have been enumerated up to size $L = 17$ [16], and on L^3 cube up to $L = 4$ [17], which is not sufficient to draw solid conclusions about asymptotic behavior for long compact chains (therefore approximate techniques, such as Monte Carlo algorithms [18, 19] have been used). In addition to the HWs enumeration, solving the semi-flexible HW problem requires their classification according to the number of bends, which makes it even less feasible. On the other hand, in real situations polymers are usually situated in nonhomogeneous media, so that models of semi-flexible compact polymers

should be extended to such environments. In that sense, as a first step towards more realistic situations, fractal lattices may be used as underlying lattices for semi-flexible HWs, which has been successfully accomplished for a broad range of polymer related problems [20–29]. Some deterministic fractal lattices have already been useful in exact studies of flexible HWs [30]. In these studies, emphasis has been put on establishing the scaling form of the number of very long walks, which is a long-standing issue in various polymer models [31]. Recently, a closely related problem of finding the scaling form of the partition function of semi-flexible HWs on 3- and 4-simplex lattices has been analyzed [32] in an exact manner. The method applied in [32] also enabled detailed analysis of various thermodynamic quantities, which brought about the conclusion that ordered crystal-like phase can not exist on these lattices. In order to resolve the question whether the inhomogeneity of the polymer environment always suppresses the crystal phase, it would be useful to extend this study on other nonhomogeneous lattices. In [33] an outline of a similar approach, applied on modified rectangular (MR) lattices, has been presented, and in this paper we generalize the applied method to the whole family of such lattices. Each member of this family is actually a square lattice with self-similarly removed bonds, where the manner in which the bonds are removed are characterized by an integer $p \geq 2$. None of the vertices is removed in this process, and fractal dimension of each of these lattices is 2, all that making them similar to the square lattice (on which most of the lattice polymer models are studied), and convenient for systematic analysis of the impact of defects in homogeneous environments on thermodynamic properties of the studied model.

The paper is organized as follows. In section 2 we describe the MR lattices for general scaling parameter p , then we introduce the model of semi-flexible HWs and the recurrence relations method for the exact evaluation of the partition function. In the same section we present specific results obtained for $p = 2$ MR lattice, and we analyze thermodynamic quantities concerning the studied model. In section 3 we generalize the method for lattice with arbitrary $p > 2$, and discuss the obtained general scaling form of the partition function. General thermodynamic behavior is presented in section 4, and the possibility of existence of different phases within the model is discussed. The behavior of the studied polymer model at temperature $T = 0$ (ground state) is examined in section 5. Summary of the obtained results and pertinent conclusions are given in section 6.

2. Semi-flexible closed HWs on the family of MR lattices

In this section the method of recurrence relations for studying the conformational properties of compact semi-flexible polymers is described. Polymer rings are modeled by closed HWs (Hamiltonian cycles), whereas the substrates on which the polymers are adsorbed are represented by fractals belonging to the MR family of fractals [34]. Members of MR fractal family are labeled by an integer p ($2 \leq p < \infty$), and can be constructed iteratively. For each particular p , at the first stage ($r = 1$) of the construction one has four points forming a unit square. Then, p unit squares are joined in the rectangle to obtain the ($r = 2$) construction stage. In the next step, p rectangles are joined into a square, and so on (see figure 1). The complete lattice is acquired in the limit $r \rightarrow \infty$. The lattice structure obtained in the r th stage is called the r th order fractal generator. It contains $N_r = 4p^{r-1}$ lattice sites, and fractal dimension is $d_f = 2$ for each fractal of the family.

To take into account the polymer stiffness property, to each bend of the walk we assign the weight factor $s = e^{-\varepsilon/k_B T}$ (stiffness parameter), where $\varepsilon > 0$ is the bending energy, T is the temperature, and k_B is the Boltzmann constant. Varying T and/or ε , the stiffness parameter can take values in the range $0 \leq s \leq 1$, where two opposite limits $s = 0$ and $s = 1$ coincide

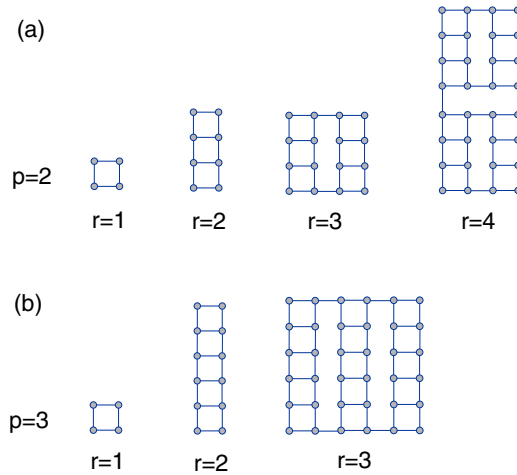


Figure 1. (a) First four steps of iterative construction of $p = 2$ MR fractal lattice. (b) First three steps in construction of $p = 3$ MR fractal.

with a fully rigid and a fully flexible polymer chain, respectively. To evaluate the partition function one has to sum the weights of all possible polymer conformations \mathcal{C}_N with N -steps: $Z_N = \sum_{\mathcal{C}_N} e^{-E(\mathcal{C}_N)/k_B T}$, where $E(\mathcal{C}_N) = \varepsilon N_b(\mathcal{C}_N)$ is the energy of an N -step conformation having N_b bends. The above partition function can be written as $Z_N = \sum_{\mathcal{C}_N} s^{N_b(\mathcal{C}_N)} = \sum_{N_b} g_{N,N_b} s^{N_b}$, where g_{N,N_b} is the number of N -step conformations with N_b bends (i.e. degeneracy of the energy level εN_b).

2.1. Recursion relations construction for $p = 2$ MR lattice

To calculate the partition function for the model under study, one has to enumerate all possible Hamiltonian cycle conformations. In general, this appears to be a very complicated task, but in this case the self-similarity of MR lattices allows systematic enumeration using an exact recursive method [33]. In order to explain this approach we present its application in the case of $p = 2$ MR lattice. In figure 2(a) an example of closed HW on the $p = 2$ MR lattice of order $r = 5$ is shown. Performing a coarse-graining process one notices in figure 2(b) that this walk can be decomposed into several parts corresponding to constitutive second order generators, which consist of one or two strands. As it can be seen in figures 2(c) and (d), this process can be repeated two more times, leading to a coarse-grained HW consisting of two one-strand parts within the two constituent $r = 4$ generators. It is quite obvious that figure 2(d) is general in the sense that any closed HW on generator of any order $(r + 1)$ can be decomposed into two open HWs, traversing the two constituent r th order generators. These two open HWs are of the same type, by which we mean that both of them enter and exit the r th order generator through vertices lying at the ends of the same longer edge of the generator, perpendicularly to that edge. We denote such conformations as B_1 -type HWs, and assign to them the function

$$B_1^{(r)}(s) = \sum_{N_b} \mathcal{B}_{1,N_b}^{(r)} s^{N_b}, \quad (2.1)$$

where $\mathcal{B}_{1,N_b}^{(r)}$ is the overall number of B_1 -type HWs with N_b bends, which traverse an r th order generator. Then, knowing $B_1^{(r)}(s)$, one can calculate the partition function

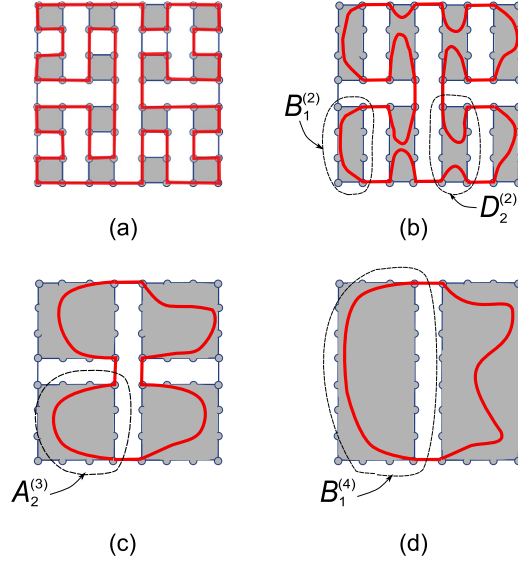


Figure 2. (a) Example of a semi-flexible Hamiltonian walk on the 5th order generator of $p = 2$ MR lattice. This walk has 42 bends, so that its statistical weight is equal to $e^{-42\epsilon/k_b T} = s^{42}$. Subsequent steps of the coarse-graining process are depicted in (b)–(d). Grey rectangles in (b)–(d) represent generators of order two, three and four, respectively, whereas curved lines correspond to the coarse grained parts of the walk. Different types of conformations within the $r = 2, 3$ and 4 generators are encircled. In (d) one can see that this closed Hamiltonian walk, observed on $r = 5$ generator, consists of two B_1 -type HWs which span the two constituent $r = 4$ generators. It is obvious that such decomposition of any closed Hamiltonian walk on generator of order $(r + 1)$ into the parts within the constituent r th order generators is the only possible one.

$$Z_c^{(r+1)} = \left(B_1^{(r)}\right)^2, \quad (2.2)$$

corresponding to all closed semi-flexible HWs on $(r + 1)$ th order lattice structure. The function $B_1^{(r)}(s)$ can be calculated recursively, utilizing the fact that each B_1 -type HW on any r th order generator can be decomposed into parts within the constituent $(r - 1)$ th generators (as depicted in figure 2(c)), and so on. As one continues HW decomposition into parts within lower order generators, careful inspection shows that altogether nine types of semi-flexible HW conformations can emerge, 5 one-stranded and 4 two-stranded (see figure 3), which differ by directions of the outer entering and exiting steps, as well as by the main direction of their strands within the generator (which can be either along longer or shorter edge). We denote these nine ‘traversing’ types of conformations as $A_1, A_2, B_1, B_2, B_3, D_1, D_2, E_1$ and E_2 , and to each of them (as for the B_1 -type) we assign a function

$$X^{(r)}(s) = \sum_{N_b} \mathcal{X}_{N_b}^{(r)} s^{N_b}, \quad X \in \{A_1, A_2, B_1, B_2, B_3, D_1, D_2, E_1, E_2\}, \quad (2.3)$$

with $\mathcal{X}_{N_b}^{(r)}$ being the number of HWs of the type X with N_b bends, on the r th order fractal structure. These functions can be thought of as restricted partition functions, and due to the self-similarity of the lattice, they obey the following recursion relations

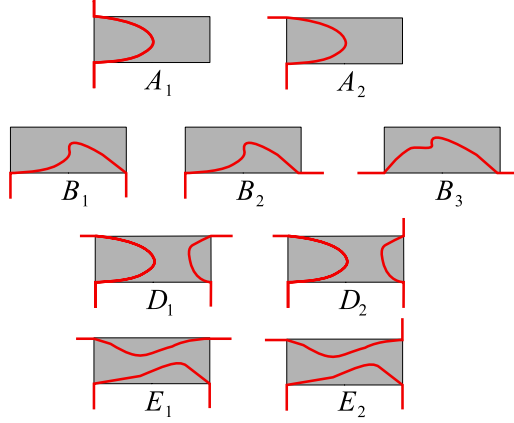


Figure 3. Possible types of semi-flexible HWs on the r th order lattice structure in the case $p = 2$.

$$\begin{aligned}
 A_1^{(r+1)} &= B_1^{(r)} D_1^{(r)}, & A_2^{(r+1)} &= B_1^{(r)} D_2^{(r)}, \\
 B_1^{(r+1)} &= \left(A_2^{(r)}\right)^2, & B_2^{(r+1)} &= A_1^{(r)} A_2^{(r)}, & B_3^{(r+1)} &= \left(A_1^{(r)}\right)^2, \\
 D_1^{(r+1)} &= 2E_2^{(r)} D_2^{(r)} + \left(B_2^{(r)}\right)^2, & D_2^{(r+1)} &= D_2^{(r)} E_1^{(r)} + E_2^{(r)} D_1^{(r)} + B_2^{(r)} B_3^{(r)}, \\
 E_1^{(r+1)} &= \left(D_2^{(r)}\right)^2, & E_2^{(r+1)} &= D_1^{(r)} D_2^{(r)}.
 \end{aligned} \tag{2.4}$$

Starting with their values for $r = 1$: $A_1^{(1)} = s^4$, $A_2^{(1)} = s^3$, $B_1^{(1)} = s^2$, $B_2^{(1)} = s^3$, $B_3^{(1)} = s^4$, $D_1^{(1)} = s^2$, $D_2^{(1)} = s$, $E_1^{(1)} = s^2$, and $E_2^{(1)} = s^3$, for any particular value of s one can, in principle, numerically find the values of the restricted partition functions for very large r values. In figure 4, construction of recursion relations for A - and B -type restricted partition functions, together with their initial conditions, is illustrated. In a similar way one can find recursive relations for the two-stranded partition functions, and the corresponding initial conditions.

Iterating restricted partition functions and using (2.2), one can obtain Z_c and, consequently, explore the thermodynamic behavior of the model. However, applying the recursion relations (2.4) for various values of s (between 0 and 1), one can show that there is a critical value of the bending parameter $s^* = 0.7366671$, such that for $s < s^*$ all restricted partition functions tend to 0 (and so does the overall partition function), whereas for $s > s^*$ they all become infinitely large, for $r \gg 1$. This can be explained by the coupling between the degeneracy g_{N,N_b} of energy levels $E(N_b) = \varepsilon N_b$ and the corresponding Boltzmann factor s^{N_b} . Degeneracies are such that they increase with the energy of levels attaining their maximum value, after which they decrease. At low temperatures (that is, for small s), degeneracies are not large enough to overcome small Boltzmann factors, but increasing the temperature they prevail and partition function iterates to infinity.

The fact that for $s > s^*$ restricted partition functions indefinitely grow makes the analysis of the thermodynamic behavior difficult, and therefore it is useful to introduce rescaled variables

$$x^{(r)} = \frac{X^{(r)}}{E_1^{(r)}}, \quad x \in \{a_1, a_2, b_1, b_2, b_3, d_1, d_2, e_2\}. \tag{2.5}$$

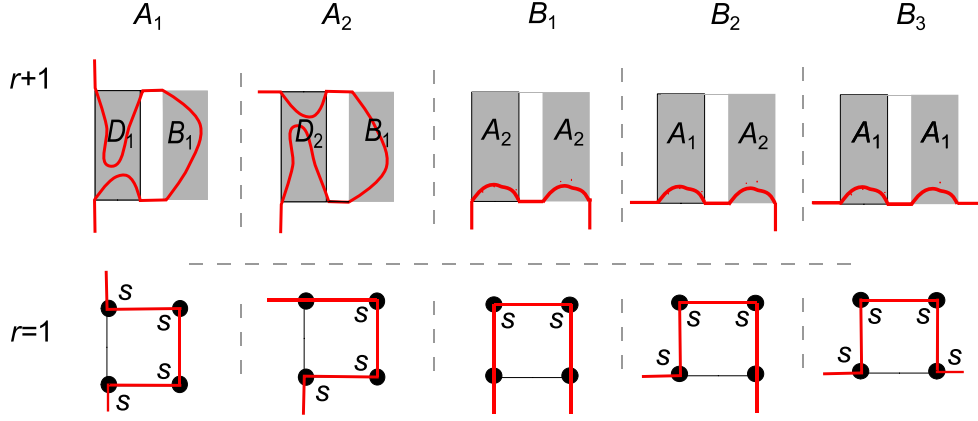


Figure 4. Top row: possible conformations of one-stranded types of semi-flexible HWs on the generator of order $(r + 1)$. Gray rectangles represent the r th order lattice structure, and curved lines correspond to coarse-grained walks. Bottom row: possible one-stranded semi-flexible HWs on the first order generator. Small black circles represent sites the lattice consists of.

These new variables fulfil the following recursion relations

$$\begin{aligned}
 a_1^{(r+1)} &= \frac{b_1^{(r)} d_1^{(r)}}{(d_2^{(r)})^2}, & a_2^{(r+1)} &= \frac{b_1^{(r)}}{d_2^{(r)}}, & e_2^{(r+1)} &= \frac{d_1^{(r)}}{d_2^{(r)}}, \\
 b_1^{(r+1)} &= \left(\frac{a_2^{(r)}}{d_2^{(r)}}\right)^2, & b_2^{(r+1)} &= \frac{a_1^{(r)} a_2^{(r)}}{(d_2^{(r)})^2}, & b_3^{(r+1)} &= \left(\frac{a_1^{(r)}}{d_2^{(r)}}\right)^2, \\
 d_1^{(r+1)} &= 2 \frac{e_2^{(r)}}{d_2^{(r)}} + \left(\frac{b_2^{(r)}}{d_2^{(r)}}\right)^2, & d_2^{(r+1)} &= \frac{1}{d_2^{(r)}} + \frac{e_2^{(r)} d_1^{(r)} + b_2^{(r)} b_3^{(r)}}{(d_2^{(r)})^2}, \quad (2.6)
 \end{aligned}$$

with the initial conditions

$$a_1^{(1)} = b_3^{(1)} = s^2, \quad a_2^{(1)} = b_2^{(1)} = e_2^{(1)} = s, \quad b_1^{(1)} = d_1^{(1)} = 1, \quad d_2^{(1)} = s^{-1}. \quad (2.7)$$

They are useful to operate with because it turns out that for any s in the region $0 < s \leq 1$, variables $a_i^{(r)}$ and $b_i^{(r)}$ quickly tend to 0, whereas $d_1^{(r)}$, $d_2^{(r)}$ and $e_2^{(r)}$ tend to some finite non-zero values. In particular, numerical analysis of (2.6) shows (see appendix A for some details) that

$$b_1^{(2k)}(s) \sim [\lambda_e(s)]^{2^k}, \quad b_1^{(2k+1)}(s) \sim [\lambda_o(s)]^{2^k}, \quad (2.8)$$

for $k \gg 1$, where λ_e and λ_o are finite functions of s (see figure 5).

Now, using the rescaled variable $b_1^{(r)}$, the partition function (2.2) may be written as

$$Z_c^{(r+1)} = \left(b_1^{(r)} E_1^{(r)}\right)^2, \quad (2.9)$$

so that, introducing variables

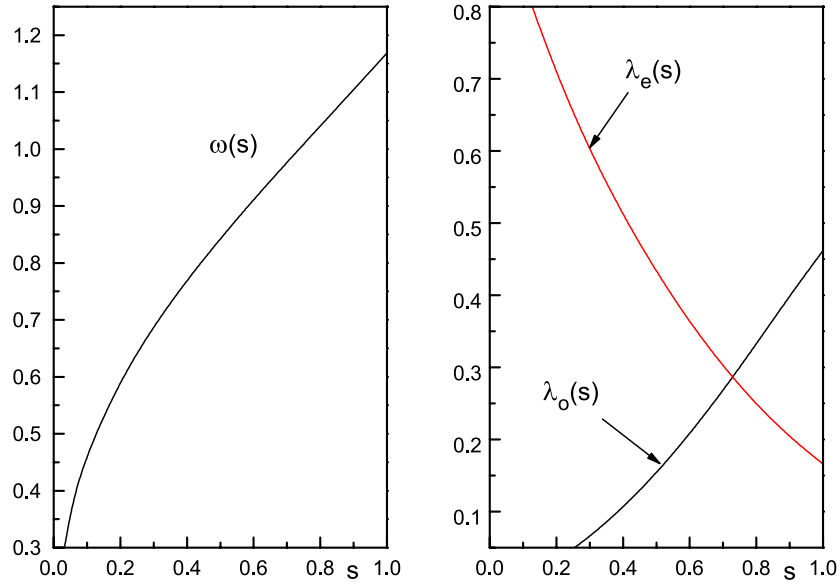


Figure 5. Dependence of ω (2.13), λ_e and λ_o (2.8) on the stiffness parameter s , for $p = 2$ MR lattice.

$$y_r = \frac{\ln Z_c^{(r)}}{N_r}, \quad q_r = \frac{\ln E_1^{(r)}}{N_r}, \quad (2.10)$$

where $N_r = 2^{r+1}$, one obtains

$$y_{r+1} = q_r + \frac{\ln b_1^{(r)}}{2^{r+1}}, \quad (2.11)$$

$$q_{r+1} = q_r + \frac{\ln d_2^{(r)}}{2^{r+1}}, \quad (2.12)$$

which follows from the recursion relation for $E_1^{(r)}$ (given in (2.4)) and definition (2.5). Numerically iterating recursion equation for q_r , for various values of s , one obtains that finite limiting value $\lim_{r \rightarrow \infty} q_r$ exists and it depends on s . Then, from (2.11) and (2.8) it follows that

$$\lim_{r \rightarrow \infty} y_r = \lim_{r \rightarrow \infty} q_r = \ln \omega(s), \quad (2.13)$$

meaning that the leading factor in the asymptotical behavior of $Z_c^{(r)}$ is ω^{N_r} . Values of $\omega(s)$ are depicted in figure 5. To find the next term in the asymptotical formula for $\ln Z_c^{(r)}$, we observe that, using (2.11)–(2.13), one obtains

$$y_{r+1} = \ln \omega + \frac{\ln b_1^{(r)}}{2^{r+1}} - \sum_{i=r}^{\infty} (q_{i+1} - q_i) = \ln \omega + \frac{\ln b_1^{(r)}}{2^{r+1}} - \sum_{i=r}^{\infty} \frac{\ln d_2^{(i)}}{2^{i+1}}. \quad (2.14)$$

Taking into account that $|\ln d_2^{(i)}|$ is less than some finite constant (which was numerically obtained), one can conclude that for $r \gg 1$ the following approximate relation follows

$$y_{r+1} \approx \ln \omega + \frac{\ln b_1^{(r)}}{2^{r+1}}. \quad (2.15)$$

Employing the relations (2.8), it further leads to the following form of the partition function:

$$Z_c^{(r)}(s) \sim [\omega(s)]^{N_r} \times \begin{cases} [\mu_e(s)]^{\sqrt{N_r}}, & \text{for } r \text{ even} \\ [\mu_o(s)]^{\sqrt{N_r}}, & \text{for } r \text{ odd} \end{cases}, \quad (2.16)$$

where $\mu_e(s) = [\lambda_o(s)]^{1/\sqrt{2}}$ and $\mu_o(s) = \lambda_e(s)$.

2.2. Thermodynamics of semi-flexible Hamiltonian cycles on $p = 2$ MR lattice

By definition, the free energy per monomer, in the thermodynamic limit, is equal to

$$f = -k_B T \lim_{r \rightarrow \infty} \frac{\ln Z_c^{(r)}}{N_r}, \quad (2.17)$$

so that, from (2.10) and (2.13), it follows

$$f = -k_B T \ln \omega = \varepsilon \frac{\ln \omega}{\ln s}. \quad (2.18)$$

Using already found values of $\omega(s)$, one can obtain $f(T)$, which is shown in figure 6.

Internal energy per monomer, in the thermodynamic limit, is equal to

$$u = \varepsilon \lim_{r \rightarrow \infty} \frac{\langle N_b^{(r)} \rangle}{N_r} = s \frac{\partial}{\partial s} (f \ln s), \quad (2.19)$$

where $N_b^{(r)}$ is the number of bends within the HW. Using (2.18) and (2.13), one obtains

$$\frac{u}{\varepsilon} = s \frac{\partial}{\partial s} (\ln \omega) = s \lim_{r \rightarrow \infty} q_r', \quad (2.20)$$

where prime denotes derivative of q_r with respect to s . The recursion relation for q_r' follows from relation (2.12) and has the form

$$q_{r+1}' = q_r' + \frac{1}{N_r} \frac{(d_2^{(r)})'}{d_2^{(r)}}, \quad (2.21)$$

whereas from (2.6) one can directly obtain recursion relations for derivatives of $x^{(r)}$ (defined by (2.5)). Iterating all these relations, internal energy u can be calculated for any particular s .

Persistence length is defined as an average number of steps between two consecutive bends

$$l_p = \lim_{r \rightarrow \infty} \frac{N_r}{\langle N_b^{(r)} \rangle} = \frac{\varepsilon}{u}, \quad (2.22)$$

and can be evaluated directly from u .

Using expressions obtained for u , one can show that the heat capacity per monomer $c = \frac{\partial u}{\partial T}$ is equal to

$$c = k_B \ln^2 s \left[\frac{u}{\varepsilon} + s^2 \frac{\partial^2}{\partial s^2} (\ln \omega) \right]. \quad (2.23)$$

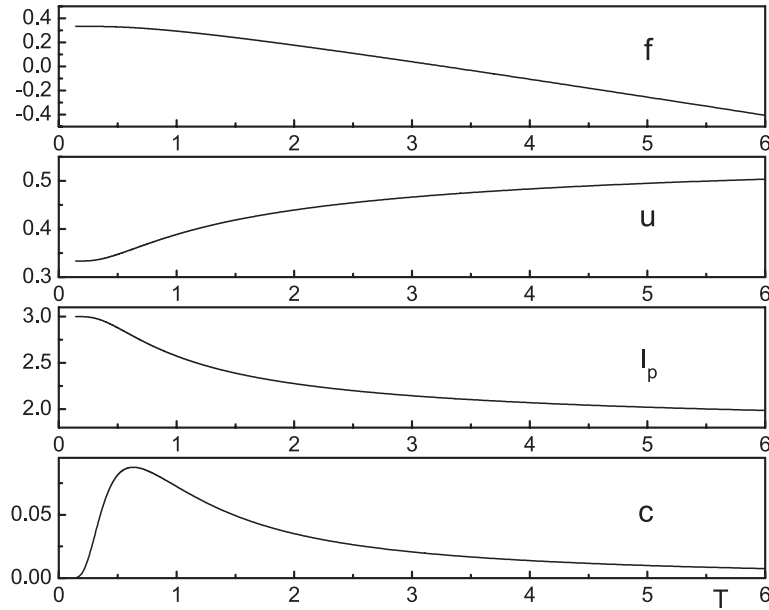


Figure 6. Free energy f (2.18), internal energy u (2.20), persistence length l_p (2.22), and heat capacity c (2.23) per monomer, in the thermodynamic limit, as functions of temperature T (f and u are measured in units of ε , c in units of k_B , and T in units of ε/k_B), for $p = 2$ MR lattice.

Since $\ln \omega = \lim_{r \rightarrow \infty} q_r$, this means that in order to calculate the heat capacity, in addition to already calculated u , one needs second derivatives of q_r , for $r \gg 1$. These derivatives can be obtained recursively using the relation

$$q''_{r+1} = q''_r + \frac{1}{N_r} \left[\frac{\left(d_2^{(r)} \right)''}{d_2^{(r)}} - \left(\frac{\left(d_2^{(r)} \right)'}{d_2^{(r)}} \right)^2 \right], \quad (2.24)$$

which follows directly from (2.21), together with recursion relations (2.6) for $x^{(r)}$ and corresponding recursive relations for their first and the second derivatives, which can be obtained straightforwardly. Temperature dependence of all evaluated thermodynamic quantities is depicted in figure 6, whereupon one can perceive that the free energy f and the persistence length of the polymer monotonically decrease with T , whereas the internal energy u is monotonically increasing function of T . Finally, the specific heat c is a non-monotonic function of temperature, displaying a maximum for some $T < 1$ (in the units of ε/k_B). These results imply that there is no finite order phase transition for the studied model. On the other hand, since for $s < s^*$ all restricted partition functions tend to 0, and for $s > s^*$ they tend to infinity, one could have expected different phases in these two regions, and therefore, existence of a phase transition. However, different polymer phases are characterized by different typical conformations. Here, that would be manifested by different mutual relationships between various restricted partition functions in the regions $s < s^*$ and $s > s^*$, but our precise and detailed numerical analysis could not detect any of these. This means that, formally speaking, structure of the recursion relations (2.4), together with their initial conditions (which are both determined by

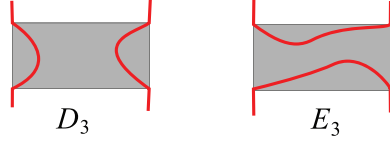


Figure 7. Two additional types of semi-flexible HWs on the r th order fractal structure, for any $p > 2$ MR lattice. Other possible conformations are of the same type as for $p = 2$ MR lattice, and they are depicted in figure 3.

the lattice topology and by the studied model) suppress abrupt change in orientational ordering of typical HW conformations, at any s value.

3. Generalization to MR lattices with $p > 2$

It is straightforward to generalize the method for lattices with $p > 2$. Due to the connectivity of the lattices and symmetry considerations, it follows that for any $p > 2$ there can be altogether eleven possible types of semi-flexible conformations. The nine ones, shown in figure 3, have already been introduced in the case of $p = 2$. Two additional ones needed in the case of $p > 2$ are shown in figure 7. In the upper part of figure 8 the only possible decomposition of any closed HW is shown, so that one concludes that the partition function of all closed semi-flexible conformations on the generator of order $(r + 1)$, for an arbitrary $p > 2$ member of the MR family, can be written as

$$Z_c^{(r+1)} = \left(B_1^{(r)}\right)^2 \left(D_3^{(r)}\right)^{p-2}. \quad (3.1)$$

Therefore, in a similar manner as in the case $p = 2$, one can iteratively calculate $Z_c^{(r+1)}$ for any r , which requires recursion relations for all eleven restricted partition functions. These relations have the following form

$$\begin{aligned} A_1^{(r+1)} &= B_1^{(r)} D_1^{(r)} \left(D_3^{(r)}\right)^{p-2}, & A_2^{(r+1)} &= B_1^{(r)} D_2^{(r)} \left(D_3^{(r)}\right)^{p-2}, \\ B_1^{(r+1)} &= \left(A_1^{(r)}\right)^{p-2} \left(A_2^{(r)}\right)^2, & B_2^{(r+1)} &= \left(A_1^{(r)}\right)^{p-1} A_2^{(r)}, & B_3^{(r+1)} &= \left(A_1^{(r)}\right)^p, \\ D_1^{(r+1)} &= 2D_2^{(r)} \left(D_3^{(r)}\right)^{p-2} E_2^{(r)} + (p-2) \left(D_2^{(r)}\right)^2 \left(D_3^{(r)}\right)^{p-3} E_3^{(r)} \\ &\quad + 2B_1^{(r)} B_2^{(r)} D_2^{(r)} \left(D_3^{(r)}\right)^{p-3} + (p-3) \left(B_1^{(r)}\right)^2 \left(D_2^{(r)}\right)^2 \left(D_3^{(r)}\right)^{p-4}, \\ D_2^{(r+1)} &= D_2^{(r)} \left(D_3^{(r)}\right)^{p-2} E_1^{(r)} + D_1^{(r)} \left(D_3^{(r)}\right)^{p-2} E_2^{(r)} + (p-2) D_1^{(r)} D_2^{(r)} \left(D_3^{(r)}\right)^{p-3} E_3^{(r)} \\ &\quad + B_1^{(r)} B_3^{(r)} D_2^{(r)} \left(D_3^{(r)}\right)^{p-3} + B_1^{(r)} B_2^{(r)} D_1^{(r)} \left(D_3^{(r)}\right)^{p-3} \\ &\quad + (p-3) \left(B_1^{(r)}\right)^2 D_1^{(r)} D_2^{(r)} \left(D_3^{(r)}\right)^{p-4}, \\ D_3^{(r+1)} &= 2D_1^{(r)} \left(D_3^{(r)}\right)^{p-2} E_1^{(r)} + (p-2) \left(D_1^{(r)}\right)^2 \left(D_3^{(r)}\right)^{p-3} E_3^{(r)} \\ &\quad + 2B_1^{(r)} B_3^{(r)} D_1^{(r)} \left(D_3^{(r)}\right)^{p-3} + (p-3) \left(B_1^{(r)}\right)^2 \left(D_1^{(r)}\right)^2 \left(D_3^{(r)}\right)^{p-4}, \\ E_1^{(r+1)} &= \left(D_2^{(r)}\right)^2 \left(D_3^{(r)}\right)^{p-2}, & E_2^{(r+1)} &= D_1^{(r)} D_2^{(r)} \left(D_3^{(r)}\right)^{p-2}, \\ E_3^{(r+1)} &= \left(D_1^{(r)}\right)^2 \left(D_3^{(r)}\right)^{p-2}. \end{aligned} \quad (3.2)$$

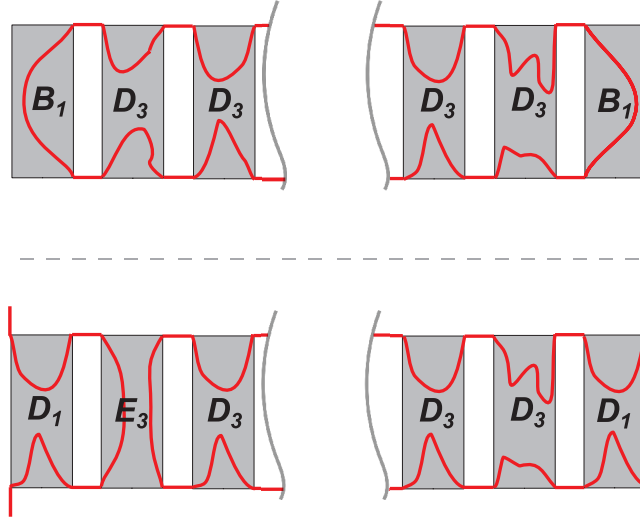


Figure 8. Upper part: decomposition of any closed semi-flexible HW on the generator of order $(r + 1)$, for an arbitrary $p > 2$ MR lattice. Grey rectangles represent p generators of order r . Lower part: example of a D_3 -type conformation on generator of order $(r + 1)$, illustrating occurrence of E_3 -type conformations on MR lattices with $p > 2$. The E_3 part can exist on any of the $(p - 2)$ inner r th order generators, so that such conformations correspond to the term $(p - 2) \left(D_1^{(r)}\right)^2 \left(D_3^{(r)}\right)^{p-3} E_3^{(r)}$ in the recursion relation for restricted partition function D_3 , given in (3.2).

The initial values for the new variables are given by $D_3^{(1)} = 1$ and $E_3^{(1)} = s^4$, while for the other variables they are the same as for the $p = 2$ case. For each restricted partition function recursion relation is obtained by decomposing the corresponding HW conformation on the generator of order $(r + 1)$ into parts within the constituent r th order generators. In the lower part of figure 8 an example of D_3 -type conformation on the generator of order $(r + 1)$ is depicted, illustrating occurrence of E_3 -type conformation. Since E_3 -type conformation within the $(r + 1)$ th order generator can traverse any of its $(p - 2)$ inner r th order generators, such conformations have overall weight equal to $(p - 2) \left(D_1^{(r)}\right)^2 \left(D_3^{(r)}\right)^{p-3} E_3^{(r)}$, which is, therefore, one of the terms in the recursion relation for restricted partition function D_3 , as can be seen in (3.2).

As in the case of $p = 2$ MR fractal, it is convenient to rescale the set of variables $X \in \{A_1, A_2, B_1, B_2, B_3, D_1, D_2, D_3, E_2, E_3\}$ by dividing them with the variable E_1 , thus introducing the new ones

$$x^{(r)} = \frac{X^{(r)}}{E_1^{(r)}}, \quad x \in \{a_1, a_2, b_1, b_2, b_3, d_1, d_2, d_3, e_2, e_3\}. \quad (3.3)$$

Then, directly from (3.2) follows that these new variables obey recurrence equation (B.1), given in appendix B, whereas the equation for E_1 becomes

$$E_1^{(r+1)} = \left(d_2^{(r)}\right)^2 \left(d_3^{(r)}\right)^{p-2} \left(E_1^{(r)}\right)^p, \quad (3.4)$$

so that the partition function (3.1) in new variables gets the form

$$Z_c^{(r+1)} = \left(b_1^{(r)}\right)^2 \left(d_3^{(r)}\right)^{p-2} \left(E_1^{(r)}\right)^p. \quad (3.5)$$

Iterating these recursion relations, one can find that, for all s values, all variables a and b tend to zero, while variables d and e tend to some finite constants, which depend on the parity of the generator order. For arbitrary p we find, similarly to equation (2.8), that b_1 approaches zero as

$$b_1^{(2k)}(s) \sim [\lambda_e(s)]^{p^k}, \quad b_1^{(2k+1)}(s) \sim [\lambda_o(s)]^{p^k}, \quad (3.6)$$

where constants λ_e and λ_o depend on the fractal parameter p . Following the same procedure as in section 2.1, for the asymptotic behavior of the partition function, for general p we again obtain the scaling form

$$Z_c^{(r)}(s) \sim [\omega(s)]^{N_r} \times \begin{cases} [\mu_e(s)]^{\sqrt{N_r}}, & \text{for } r \text{ even} \\ [\mu_o(s)]^{\sqrt{N_r}}, & \text{for } r \text{ odd} \end{cases}, \quad (3.7)$$

where now $\mu_e(s) = [\lambda_o(s)]^{1/\sqrt{p}}$ and $\mu_o(s) = \lambda_e(s)$. Dependence of ω on the stiffness parameter s , for various values of p , is given in figure 9, where one can observe that for very large p the quantity ω approaches the unit value, ceasing to depend on s . Also, one may notice that $\omega(s=1)$ is smaller for lattices with higher value of p , meaning that the number of fully flexible HWs on equally large lattices is smaller for higher p . The reason for this is that the number of edges, and therefore connectivity of lattices, decreases with p . Values of μ_e and μ_o , as functions of s , are shown in figure 10, for various values of p , where one can see that μ_e decreases, while μ_o increases with s , for each member of the MR family.

The asymptotic form (3.7) obtained for the partition function, implies that correction to the leading term in the free energy is proportional to the square root of the number of steps of the walk. This can be compared with the similar correction terms obtained for flexible compact polymers on other lattices. For homogeneous d -dimensional environments such a correction in flexible polymer models is related to surface effects, which arise due to the fact that at low temperatures a polymer forms a compact globule, whose surface is proportional to $N^{(d-1)/d}$, with N being the number of monomers in globule [35]. Results obtained for flexible HWs on some fractal lattices imply that simple generalization of such correction term for nonhomogeneous environments is not possible [30]. In particular, correction term on all studied fractal lattices is of the same form μ^{N^σ} as for regular lattices, but σ is non-universal, i.e. it depends not only on fractal dimension, but also on other lattice characteristics. Here we have found the same value $\sigma = 1/2$ for each member (with the same fractal dimension 2) of the MR fractal family, meaning that σ depends neither on parameters by which these lattices differ, nor on the stiffness parameter s . This can be compared with the results $\sigma = 0$ and $\sigma = 1/2$, obtained for semi-flexible HWs on 3- and 4-simplex fractal lattices, respectively, for all values of s [32]. To the best of our knowledge, impact of the polymer rigidity on σ in the case of semi-flexible compact polymers on homogeneous lattices has not yet been studied, but on the bases of these results one could expect that it might be universal. That would also be in accord with recent conclusion that some other critical exponents, corresponding to semi-flexible SAW on the square lattice, also do not depend on s [36].

4. Thermodynamics of semi-flexible Hamiltonian cycles for general p

Thermodynamic functions for semi-flexible Hamiltonian cycles on MR lattices with $p > 2$ may be obtained using the recurrence equation (B.1), given in appendix B and expressions

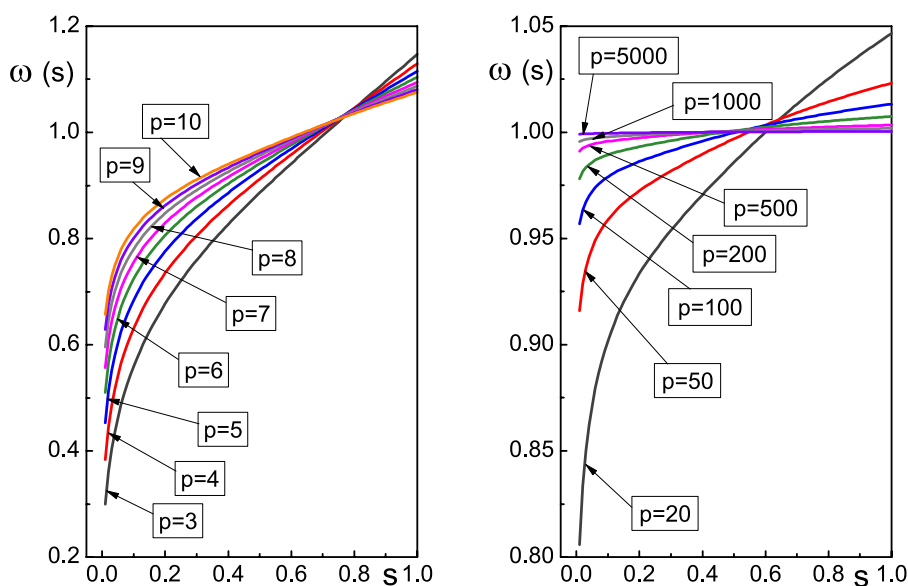


Figure 9. Stiffness dependence of the base ω in (3.7), for various members of the MR family, labelled by parameter p .

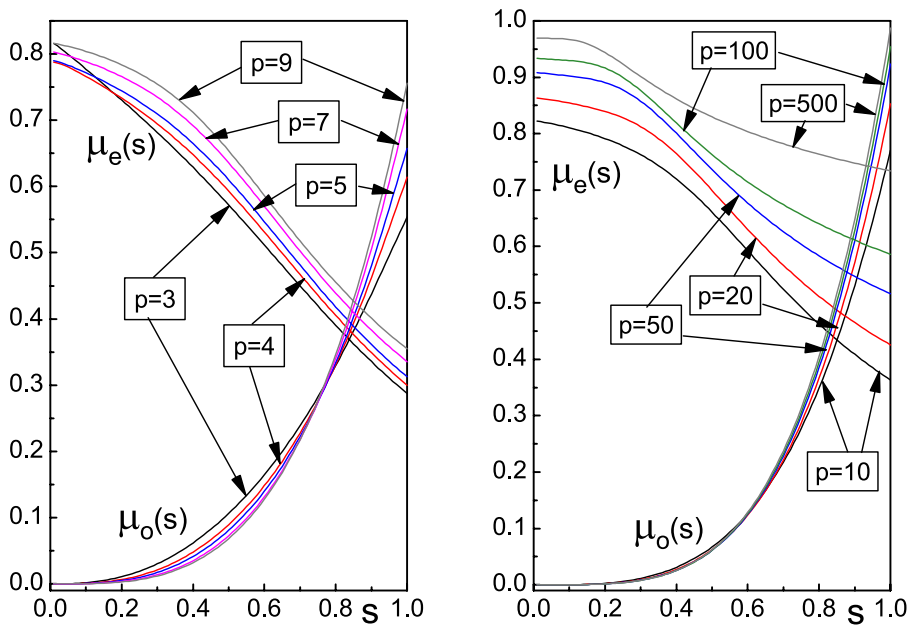


Figure 10. Stiffness dependence of the bases μ in the stretched exponential factor in (3.7), for various members of the MR family, labelled by parameter p .

$$q_{r+1} = q_r + \frac{1}{4p^r} \left(2 \ln d_2^{(r)} + (p-2) \ln d_3^{(r)} \right), \quad (4.1)$$

$$q'_{r+1} = q'_r + \frac{1}{4p^r} \left(2 \frac{(d_2^{(r)})'}{d_2^{(r)}} + (p-2) \frac{(d_3^{(r)})'}{d_3^{(r)}} \right), \quad (4.2)$$

$$q''_{r+1} = q''_r + \frac{1}{4p^r} \left[2 \frac{(d_2^{(r)})''}{d_2^{(r)}} - 2 \left(\frac{(d_2^{(r)})'}{d_2^{(r)}} \right)^2 \right] \\ + \frac{1}{4p^r} \left[(p-2) \frac{(d_3^{(r)})''}{d_3^{(r)}} - (p-2) \left(\frac{(d_3^{(r)})'}{d_3^{(r)}} \right)^2 \right], \quad (4.3)$$

that correspond to the equations (2.12), (2.21) and (2.24) (obtained for $p = 2$ case), respectively.

The obtained numerical results for the persistence length l_p as function of temperature T , for different MR fractals, are depicted in figure 11, where one can see that l_p decreases with temperature, implying that number of polymer bends increases with T . Dependence of free and internal energy on T is presented in figure 12, for various members of the MR family. One perceives that f monotonically decreases, while u monotonically increases with T , for each p . Also, in the limit of very large p , one can conclude that both f and u go to zero. The obtained increment of internal energy with temperature is in accordance with the fact that at lower temperatures energetic effects dominate, so that low energy levels with conformations consisting of smaller number of bends are more populated. At higher temperatures, all energy levels become populated and internal energy saturates (i.e. becomes constant). This saturation is faster on fractals with larger values of p , for which the internal energy is generally smaller. The reason for this lies in the connectivity of the vertices. For lattices oriented as in figure 1 there are more vertical than horizontal edges, and for lattices with larger value of p this anisotropy becomes larger. The walks follow preferred direction and make smaller number of turns which reduces energy and increases persistence length. Described behavior of internal energy implies that specific heat should have a peak in the low temperature region, which we have numerically confirmed and displayed in figures 13 and 14, where specific heat as a function of T is shown. In these figures one can notice that besides one pronounced peak in specific heat landscape, there is another small peak at low temperatures, for fractals with $p \geq 4$. This effect in specific heat behaviour is known as Schottky anomaly (see, for instance [37]) and appears in systems with a finite number of energy levels.

We finish our discussion inferring that within the studied compact polymer phase there is no finite order phase transition, due to the fact that entropy and specific heat are continuous, smooth functions of temperature. One might challenge this conclusion, because it is based on numerical calculations, however, these calculations were performed with high precision, only by iterating exact recursion relations. For instance, the free energy is obtained by calculating $\omega(s)$ (see (2.18)), which is a limiting value of variable q_r that quickly saturates upon iterations. Furthermore, calculations were performed for a large number of s values, therefore functions $f(T)$ presented in figures 6 and 12 are obtained with high accuracy and one might be pretty sure, only relying on these figures, that the free energy is a differentiable function of T . Of course, this was further confirmed by

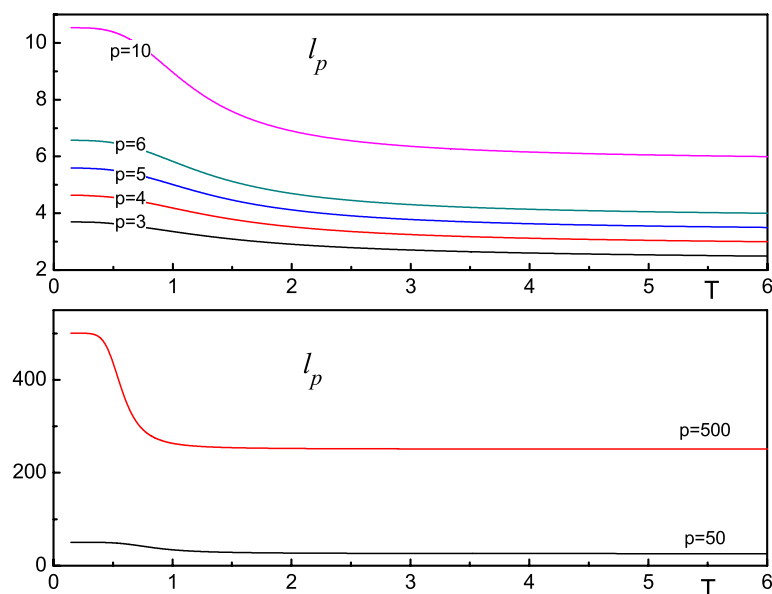


Figure 11. Persistence length l_p as a function of temperature, for various values of parameter p that enumerates members of the MR family.

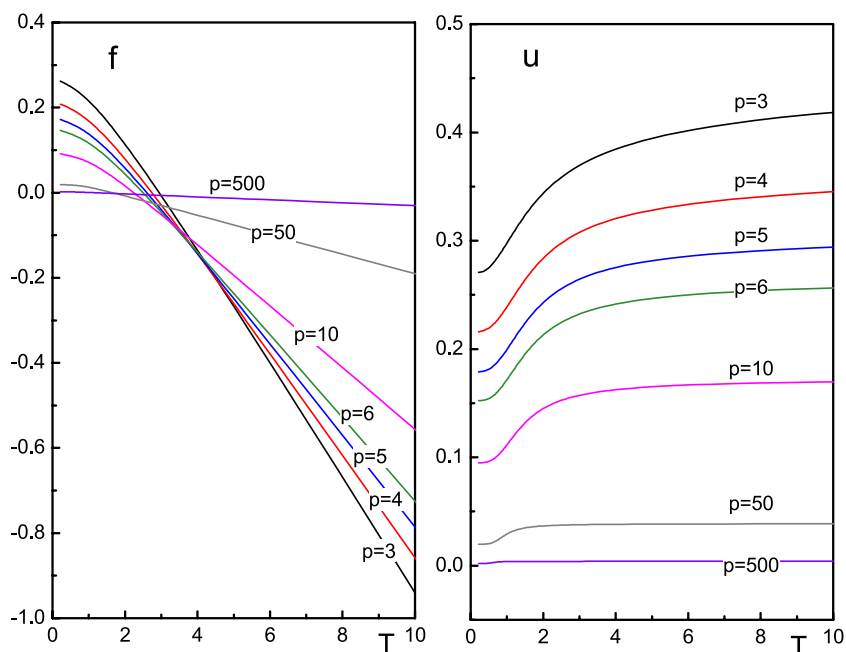


Figure 12. Free energy f and internal energy u as functions of temperature, for various values of parameter p that enumerates members of the MR family.

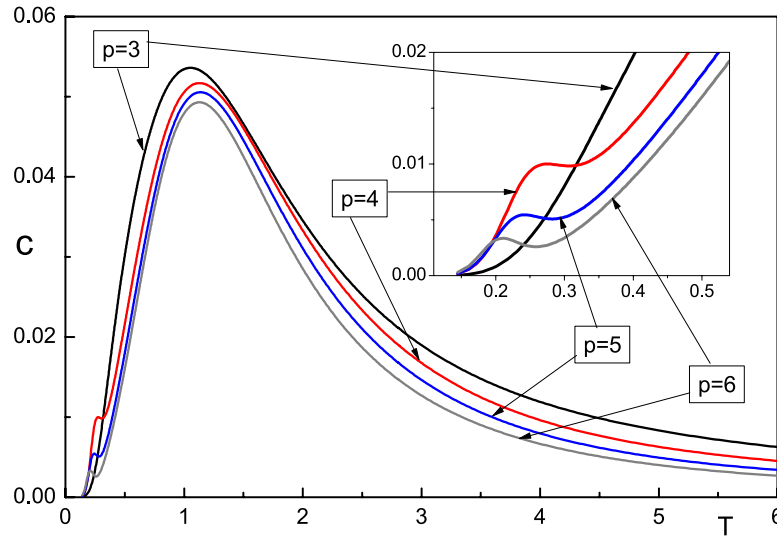


Figure 13. Specific heat c as a function of temperature T , for MR fractals labelled by $p = 3, 4, 5$, and 6 . Inset graph highlights additional small peaks that have appeared for $p = 4, 5$ and 6 fractals.

calculating the other thermodynamic functions, which, although defined through partial derivatives with respect to s , can be done without actual numerical differentiation, but again iteratively, utilizing the fact that derivatives of q_r obey recurrence relations (4.2) and (4.3). Since the persistence length l_p is finite at any T (for finite p), the polymer system is always in liquid-like (disordered) phase, and the transition to the crystal (ordered) phase is not possible. The existence of only disordered compact phase has also been observed in the case of semi-flexible HW on 3- and 4-simplex lattices [32]. The absence of crystal phase on the studied family of lattices stems from their asymmetry in horizontal and vertical direction. For each MR fractal there are more vertical than horizontal bonds. This discrepancy is more pronounced for larger p lattices, implying smaller number of bends in compact conformations since they are forced by the lattice in the vertical direction. Nevertheless, on such lattices conformations still have a large number of horizontal steps that prevent an ordered state that can exist on the square lattice [11].

5. Ground states and frustration

In order to achieve a minimal energy state at $T = 0$, in this section only conformations with a minimal number of bends will be considered. First we analyse the case of $p = 2$ lattice. Since the conformation D_2 makes the smallest number of bends on the unit square, one expects that the ground state, in this case, would be comprised of HW conformations with the maximal possible number of D_2 type on each unit square. Contribution of the ground state to the whole partition function is of the form $Z_0 = N_0 s^{N_{b0}}$, with N_0 being the number of ground state HWs and N_{b0} being the number of bends in each of these conformations. This term in the partition function can be obtained from the relation (2.2) and recurrence equation (2.4), keeping only the terms with conformations of the type D_2 . Then, some of the variables drop, and the system (2.4) reduces to

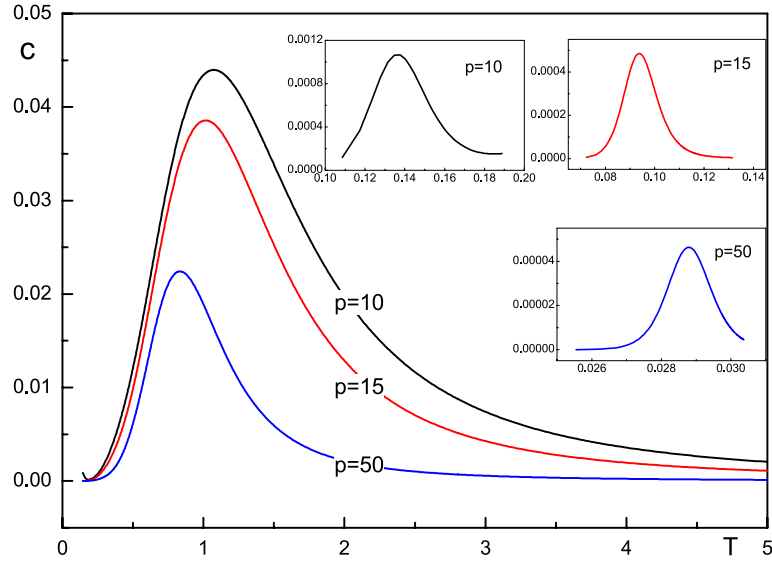


Figure 14. Specific heat as function of temperature, for $p = 10$, $p = 15$ and $p = 50$ fractals. Inset graphs show small peaks for these fractals. For higher p , peaks are smaller and pulled toward lower temperatures.

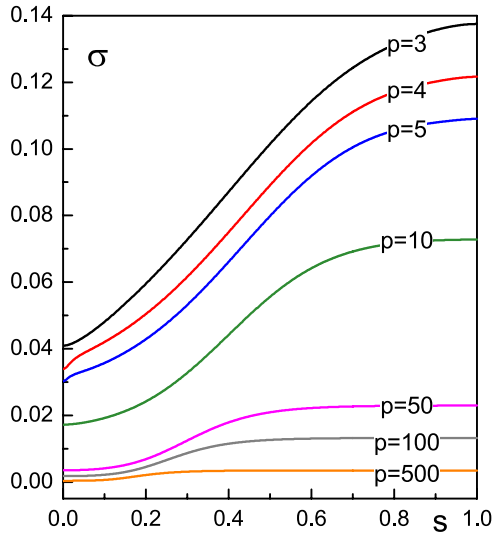


Figure 15. Entropy per monomer σ , in thermodynamic limit, as a function of the stiffness parameter s , for various members of the MR fractal family (labelled by p).

$$\begin{aligned}
 A_2^{(r+1)} &= B_1^{(r)} D_2^{(r)}, & B_1^{(r+1)} &= \left(A_2^{(r)}\right)^2, \\
 D_2^{(r+1)} &= D_2^{(r)} E_1^{(r)}, & E_1^{(r+1)} &= \left(D_2^{(r)}\right)^2.
 \end{aligned}
 \tag{5.1}$$

Solving this system exactly, from (2.2) we obtained Z_0 on the r th order fractal structure

Table 1. Entropies per monomer σ^* at temperature $T = 0$, for various p fractals of the MR family. We see that σ^* (and consequently the number of ground state conformations) decreases with p .

p	3	4	5	10	50	100	500
σ^*	0.040902	0.033925	0.030247	0.016914	0.0034679	0.0017333	0.00034658

$$Z_{0r} = s^{(\sqrt{2})^{r+1}[1+(-1)^{r+1}] + \frac{2}{3}2^r + \frac{4}{3}(-1)^r}. \quad (5.2)$$

In this case the ground state is non-degenerate, with the only one conformation leading to the zero entropy. From the number of bends in this conformation, given by $N_{b0r} = (\sqrt{2})^{r+1}[1 + (-1)^{r+1}] + \frac{2}{3}2^r + \frac{4}{3}(-1)^r$, we could calculate the ground state energy per site in the thermodynamic limit, as $u_0 = \varepsilon \lim_{r \rightarrow \infty} \frac{N_{b0r}}{2^{r+1}}$. The obtained value is $\frac{u_0}{\varepsilon} = \frac{1}{3}$, which is verified numerically and can be seen in figure 6.

For $p > 2$ equations are more complicated, and we have not been able to extract exact expressions for the number of ground state conformations, but numerically we have calculated the entropies per site, in the thermodynamic limit, in the whole range of stiffness parameter s (see figure 15). One can observe that for $p > 2$ fractals, ground state entropies per monomer do not vanish, meaning that there are exponentially large number of ground state conformations, which is a characteristic of geometrically frustrated systems. Limiting values of entropies for various MR fractals are given in table 1.

6. Summary and conclusion

We have studied a model of compact semi-flexible polymer rings modelled by closed HWs on the family of MR fractal lattices, whose members are labelled by an integer $p \geq 2$. All lattices from the family have the same fractal dimension ($d_f = 2$) and the coordination number (three), but their vertices are connected differently. Lattices can be obtained from the square lattice by deleting some bonds from it, which induces anisotropy between horizontal and vertical direction. By applying an exact method of recurrence relations, we have established the scaling form of the corresponding partition function (given by equation (3.7)) on the whole family of fractals. There is a leading exponential factor with a base ω , which depends on the lattice parameter p , as well as on the stiffness parameter s . For each p studied, we have found numerically that ω is increasing function of s , and that it changes more slowly on fractals with higher p . Correction to the leading exponential factor is stretched exponential factor of the same form for each fractal of the considered family, in the whole range of s values.

From the obtained partition function we have evaluated the set of thermodynamic quantities (free and internal energy, specific heat and entropy) as well as the polymer persistence length, as functions of the stiffness parameter s (or temperature T). We have found that all these quantities are differentiable functions of s . For each member of the MR family, we have found that all these quantities are monotonic functions of T , except for the specific heat, which has a maximum at low temperatures. Since the entropy and specific heat are continuous, smooth functions of temperature, there is no finite order phase transition, and the studied polymer system can exist only in disordered phase.

Eventually, we have analysed the ground state of the studied model. For $p = 2$ fractal we have found that the ground state is non-degenerate, and that the only ground state conformation has the persistence length $l_p = 3$. So, on average, there is one bend after every three steps, and there are no long straight segments in this conformation. The number of left/right

and up/down turns are comparable and this conformation is disordered. On the other hand, for fractals with $p > 2$, the ground state is degenerate, with exponentially large number of conformations, producing the residual entropy. The number of ground state conformations is maximal for $p = 3$ and decreases with p . Persistence length is the smallest for $p = 3$ ground state, and becomes larger, for larger p . However, all these ground state conformations have many bends and do not represent ordered ground states. In fact, we have geometrically frustrated systems, where geometry of the lattices is in conflict with the condition for minimal energy (i.e. minimal number of bends) and the requirement that all vertices are occupied only once. Geometric frustration suppresses ordered ground states and possibility of ordered phase at any T . The studied model describes disordered, liquid-like compact phase of semi-flexible polymers. Although MR lattices have some resemblance to the square lattice (on which the ordered phase can exist), an anisotropy of vertical and horizontal directions (small for $p = 2$, and greater for $p > 2$), causes that ordered phase can not exist on these lattices.

The main conclusion of this paper that inhomogeneity of the environment, in which the model was studied, suppresses the crystal phase of semiflexible polymers is in accord with the conclusions obtained in [32] for the same model applied on 3- and 4-simplex fractal lattices. Whereas there are no results for this model on homogeneous lattices that have symmetry similar to 3- and 4-simplex lattices (such as triangular or tetragonal ones), the family of MR lattices provides an infinite spectrum of nonhomogeneous lattices which differ from the square lattice by having smaller number of bonds, while the number of vertices is the same. Therefore, conclusion obtained here might imply that any kind of inhomogeneity can suppress occurring of the ordered phase. However, we think that this issue should be further inspected by performing similar studies on other nonhomogeneous lattices, and it could be of practical significance to expand the study of examined model into a more realistic case, when polymers are situated in three-dimensional fractal space.

Acknowledgments

This paper is part of the work within the project No. 171015, funded by the Ministry of Education, Science and Technological Development of the Republic of Serbia.

Appendix A

Here we give some additional details of the analysis of recursion relations (2.6) for the rescaled variables $x^{(r)}$ in the case of $p = 2$ MR lattice, given in section 2.1. For any $0 < s \leq 1$, by iterating (2.6), one obtains

$$\begin{aligned} \lim_{k \rightarrow \infty} d_1^{(2k+1)}(s) &= d_1^o(s), & \lim_{k \rightarrow \infty} d_2^{(2k+1)}(s) &= d_2^o(s), & \lim_{k \rightarrow \infty} e_2^{(2k+1)}(s) &= e_2^o(s), \\ \lim_{k \rightarrow \infty} d_1^{(2k)}(s) &= d_1^e(s), & \lim_{k \rightarrow \infty} d_2^{(2k)}(s) &= d_2^e(s), & \lim_{k \rightarrow \infty} e_2^{(2k)}(s) &= e_2^e(s), \end{aligned} \quad (\text{A.1})$$

where dependence of the limiting values $d_1^{o,e}$, $d_2^{o,e}$ and $e_2^{o,e}$ on s is depicted in figure A1.

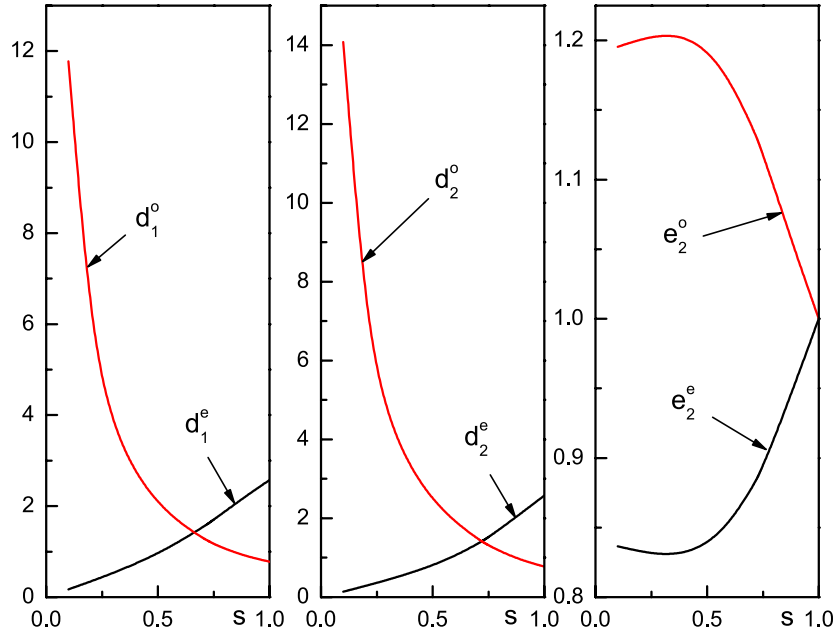


Figure A1. Dependence of the limiting values $d_1^{o,e}$, $d_2^{o,e}$ and $e_2^{o,e}$, defined in (A.1), on the stiffness parameter s , for $p = 2$ MR lattice.

Furthermore, the following relations are satisfied

$$d_2^o d_2^e = d_3^o d_3^e = 2, \quad e_2^o e_2^e = 1, \quad (\text{A.2})$$

so that using relations (2.6), for large r one obtains the asymptotic recursion relation

$$b_1^{(r+2)} \approx \frac{1}{4} \left(b_1^{(r)} \right)^2, \quad (\text{A.3})$$

which implies that

$$b_1^{(2k)}(s) \sim [\lambda_e(s)]^{2^k}, \quad b_1^{(2k+1)}(s) \sim [\lambda_o(s)]^{2^k}, \quad (\text{A.4})$$

for $k \gg 1$. Dependence of λ_e and λ_o on values of the bending parameter s , obtained by numerical iteration of $\frac{\ln b_1^{(r)}(s)}{2^{[r/2]}}$, is depicted in figure 5.

Appendix B

In this appendix we give recurrence relations for the rescaled variables $x^{(r)}$ in the case of $p > 2$ MR lattice, defined in section 3 by (3.3). Directly from recurrence relations (3.2) one obtains

$$\begin{aligned}
a_1^{(r+1)} &= \frac{b_1^{(r)} d_1^{(r)}}{(d_2^{(r)})^2}, & a_2^{(r+1)} &= \frac{b_1^{(r)}}{d_2^{(r)}}, & b_1^{(r+1)} &= \left(\frac{a_2^{(r)}}{d_2^{(r)}}\right)^2 \left(\frac{a_1^{(r)}}{d_3^{(r)}}\right)^{p-2}, \\
b_2^{(r+1)} &= \frac{a_1^{(r)} a_2^{(r)}}{(d_2^{(r)})^2} \left(\frac{a_1^{(r)}}{d_3^{(r)}}\right)^{p-2}, & b_3^{(r+1)} &= \left(\frac{a_1^{(r)}}{d_2^{(r)}}\right)^2 \left(\frac{a_1^{(r)}}{d_3^{(r)}}\right)^{p-2}, \\
d_1^{(r+1)} &= 2 \frac{e_2^{(r)}}{d_2^{(r)}} + (p-2) \frac{e_3^{(r)}}{d_3^{(r)}} + 2 \frac{b_1^{(r)} b_2^{(r)}}{d_2^{(r)} d_3^{(r)}} + (p-3) \left(\frac{b_1^{(r)}}{d_3^{(r)}}\right)^2, \\
d_2^{(r+1)} &= \frac{1}{d_2^{(r)}} + \frac{d_1^{(r)} e_2^{(r)}}{(d_2^{(r)})^2} + \frac{(p-2) d_1^{(r)} e_3^{(r)} + b_1^{(r)} b_3^{(r)}}{d_2^{(r)} d_3^{(r)}} + \frac{b_1^{(r)} b_2^{(r)} d_1^{(r)}}{(d_2^{(r)})^2 d_3^{(r)}} + (p-3) \frac{(b_1^{(r)})^2 d_1^{(r)}}{d_2^{(r)} (d_3^{(r)})^2}, \\
d_3^{(r+1)} &= 2 \frac{d_1^{(r)}}{(d_2^{(r)})^2} + (p-2) \frac{(d_1^{(r)})^2 e_3^{(r)}}{(d_2^{(r)})^2 d_3^{(r)}} + 2 \frac{b_1^{(r)} b_3^{(r)} d_1^{(r)}}{(d_2^{(r)})^2 d_3^{(r)}} + (p-3) \frac{(b_1^{(r)})^2 (d_1^{(r)})^2}{(d_2^{(r)})^2 (d_3^{(r)})^2}, \\
e_2^{(r+1)} &= \frac{d_1^{(r)}}{d_2^{(r)}}, & e_3^{(r+1)} &= \left(\frac{d_1^{(r)}}{d_2^{(r)}}\right)^2.
\end{aligned} \tag{B.1}$$

ORCID iDs

S Elezović-Hadžić  <https://orcid.org/0000-0001-8148-5828>

References

- [1] de Gennes P-G 1979 *Scaling Concepts in Polymer Physics* (Ithaca, NY: Cornell University Press)
- [2] Vanderzande C 1998 *Lattice Models of Polymers* (Cambridge: Cambridge University Press)
- [3] Flory P J 1956 *Proc. R. Soc. A* **234** 60
- [4] Gujrati P D 1980 *J. Phys. A: Math. Gen.* **13** L437
- [5] Saleur H 1986 *J. Phys. A: Math. Gen.* **19** 2409
- [6] Baumgartner A and Yoon D L 1983 *J. Chem. Phys.* **79** 521
- [7] Doniach S, Garel T and Orland H 1996 *J. Chem. Phys.* **105** 1601
- [8] Irbäck A and Sandelin E 1999 *J. Chem. Phys.* **110** 12256
- [9] Dijkstra M and Frenkel D 1994 *Phys. Rev. E* **50** 349
- [10] Gujrati P D and Corsi A 2001 *Phys. Rev. Lett.* **87** 025701
Corsi A and Gujrati P D 2003 *Phys. Rev. E* **68** 031502
- [11] Jacobsen J L and Kondev J 2004 *Phys. Rev. E* **69** 066108
Jacobsen J L and Kondev J 2004 *Phys. Rev. Lett.* **92** 210601
- [12] Krawczyk J, Owczarek A L and Prellberg T 2009 *Physica A* **388** 104
Krawczyk J, Owczarek A L and Prellberg T 2010 *Physica A* **389** 1619
- [13] Starostin E L 2013 *J. Chem. Phys.* **138** 164903
- [14] Karshikoff A, Nilsson L and Ladenstein R 2015 *FEBS J.* **282** 3899
- [15] Nuebler J, Fudenberg G, Imakaev M, Abdennura N and Mirny L A 2018 *Proc. Natl Acad. Sci.* **115** 6697
- [16] Jacobsen J L 2007 *J. Phys. A: Math. Theor.* **40** 14667
- [17] Schram R D and Schiessel H 2013 *J. Phys. A: Math. Theor.* **46** 485001
- [18] Oberdorf R, Ferguson A, Jacobsen J L and Kondev J 2006 *Phys. Rev. E* **74** 051801
- [19] Jacobsen J L 2008 *Phys. Rev. Lett.* **100** 118102
- [20] Dhar D and Singh Y 2005 Linear and branched polymers on fractals *Statistics of Linear Polymers in Disordered Media* ed B K Chakrabarti (Amsterdam: Elsevier)

- [21] Giacometti A and Maritan A 1992 *J. Phys. A: Math. Gen.* **25** 2753
- [22] Živić I, Milošević S and Stanley E H 1994 *Phys. Rev. E* **49** 636
- [23] Marenduzzo D, Maritan A and Seno F 2002 *J. Phys. A: Math. Gen.* **35** L233
- [24] Dhar D 2005 *Phys. Rev. E* **71** 031801
- [25] Vidanović I, Arsenijević S and Elezović-Hadžić S 2011 *Eur. Phys. J. B* **81** 291
- [26] Pretti M 2016 *Phys. Rev. E* **93** 032110
- [27] Maji J, Seno F, Trovato A and Bhattacharjee S M 2017 *J. Stat. Mech.* **073203**
- [28] Cheraghalizadeh J, Najafi M N, Mohammadzadeh H and Saber A 2018 *Phys. Rev. E* **97** 042128
- [29] Oliveira T J, Dantas W G, Prellberg T and Stilck J F 2018 *J. Phys. A: Math. Theor.* **51** 054001
- [30] Bradley R M 1989 *J. Phys. A: Math. Gen.* **22** L19
- Stajić J and Elezović-Hadžić S 2005 *J. Phys. A: Math. Gen.* **38** 5677
- Elezović-Hadžić S, Marčetić D and Maletić S 2007 *Phys. Rev. E* **76** 011107
- Lekić D and Elezović-Hadžić S 2010 *J. Stat. Mech.* **P02021**
- [31] Roy A K and Chakrabarti B K 1987 *J. Phys. A: Math. Gen.* **20** 215
- Blavatska V and Janke W 2009 *J. Phys. A: Math. Theor.* **42** 015001
- Fricke N and Janke W 2014 *Phys. Rev. Lett.* **113** 255701
- Fricke N and Janke W 2017 *J. Phys. A: Math. Theor.* **50** 264002
- [32] Lekić D and Elezović-Hadžić S 2011 *Physica A* **390** 1941
- [33] Lekić D, Elezović-Hadžić S and Adžić N 2016 *Contemp. Mater.* **VII-2** 166 (*Conference Paper in IX Int. Scientific Conf. Contemporary Materials 2016, Banja Luka: Academy of Sciences and Arts of the Republic of Srpska*)
- [34] Dhar D 1978 *J. Math. Phys.* **18** 577
- Dhar D 1978 *J. Math. Phys.* **19** 5
- Dhar D and Vannimenus J 1978 *J. Phys. A: Math. Gen.* **20** 199
- [35] Owczarek A L, Prellberg T and Brak R 1993 *Phys. Rev. Lett.* **70** 951
- Duplantier B 1993 *Phys. Rev. Lett.* **71** 4274
- Grassberger P and Hsu H P 2002 *Phys. Rev. E* **65** 031807
- Baiesi M, Orlandini E and Stella A L 2007 *Phys. Rev. Lett.* **99** 058301
- Baiesi M and Orlandini E 2014 *Phys. Rev. E* **89** 062601
- [36] Živić I, Elezović-Hadžić S and Milošević S 2018 *Phys. Rev. E* **98** 062133
- [37] Tari A 2003 *The Specific Heat of Matter at Low Temperatures* (London: Imperial College Press)